
ELEMENTARY PARTICLES AND FIELDS
Experiment

**Elimination of Diurnal, Annual, and Solar Variations
in the Matrix Observations of the URAGAN Muon Hodoscope**

**I. I. Astapov^{1),2)}, A. D. Gvishiani^{1),3)}, V. G. Getmanov^{1),3)},
A. N. Dmitrieva^{1),2)}, M. N. Dobrovolsky¹⁾, A. A. Kovylyayeva^{1),2)},
R. V. Sidorov^{1)*}, A. A. Soloviev^{1),3)}, V. E. Chinkin^{1),4)}, and I. I. Yashin^{1),2)}**

Received July 25, 2019; revised July 25, 2019; accepted July 25, 2019

Abstract—A method for elimination of periodical diurnal, annual, and 27-day and 11-year solar variations in the matrix observations of the URAGAN muon hodoscope was developed. The analysis of the parameters of these variations in the time and frequency domains was performed. Two-dimensional bandpass filtering of sequences of muon hodoscope matrix observations was implemented. The structure of a two-dimensional filter is developed, based on the operation of elementwise matrix multiplications and additions. Examples of eliminating variations in the URAGAN muon hodoscope matrix observations are discussed.

DOI: 10.1134/S1063778819660050

1. INTRODUCTION

The elimination of periodic components in the sequences of matrix observations is in demand for many applications of experimental physics related to the separation of processes of different scales in time and space. For example, this procedure is applied: in the analysis of periodical secular and seasonal processes of ice formation in the polar regions; in considering the effect of cyclic solar activity on slow climatic changes in given regions of the Earth's surface; in separation of tidal modulations and sea level wind surges in aerial photographs, etc. Here an application is discussed, related to the task of processing the periodical muon fluxes (MF) variations in the URAGAN MH [1, 2] matrix observation data. Two-dimensional filtering, implemented here, refers to the growing field of digital signal processing [3, 4].

MF, reaching the MH aperture-type detector, are subject to temporal and spatial variations [5] which can be divided into: periodical, related to the Earth's daily rotation; annual, caused by the Earth's motion in the solar orbit; solar—due to the 11-year activity cycle and the 27-day one caused by the Sun's rotation [6]; and aperiodical, from Forbush decreases

[7] and the atmosphere's impact [8, 9]. This article substantially developed the results described in the publication [10].

2. MH DATA ANALYSIS IN TEMPORAL AND SPATIAL DOMAINS

The judgment on diurnal, 27-day, annual and 11-year components in matrix data from MH can be made based on temporal and spectral analysis of MH data.

2.1. Spatial Domain Analysis

Let us analyze the oscillatory components in the data from MH using the temporal domain analysis. Let $M_a(i, j, Tk)$ be the sequence of matrix hourly data, where $i = 1, \dots, N_1, j = 1, \dots, N_2$, and N_1, N_2 are the MH aperture-type detector dimensions, and $k = 1, \dots, k_f$ represents the time interval. We introduce the averaged muon flux intensity $S(Tk)$, whose physical significance is obvious:

$$S(Tk) = \frac{1}{N_1 N_2} \sum_{i=1}^{N_1} \sum_{j=1}^{N_2} M_a(i, j, Tk),$$

$$k = 1, \dots, k_f.$$

On Fig. 1, the function $S(Tk)$ is presented, made from the data from MH during February 6, 2007, 11:00 UT–December 31, 2018, 23:00 UT. The mentioned period corresponds to a 12-year observation interval, approximately; the number of observations $k_f = 105320$. From this figure, the annual (seasonal)

¹⁾Geophysical Center of the Russian Academy of Sciences, Moscow, Russia.

²⁾National Research Nuclear University MEPhI, Moscow, Russia.

³⁾Schmidt Institute of Physics of the Earth of the Russian Academy of Sciences, Moscow, Russia.

⁴⁾Bauman Moscow State Technical University, Moscow, Russia.

*E-mail: r.sidorov@gcras.ru

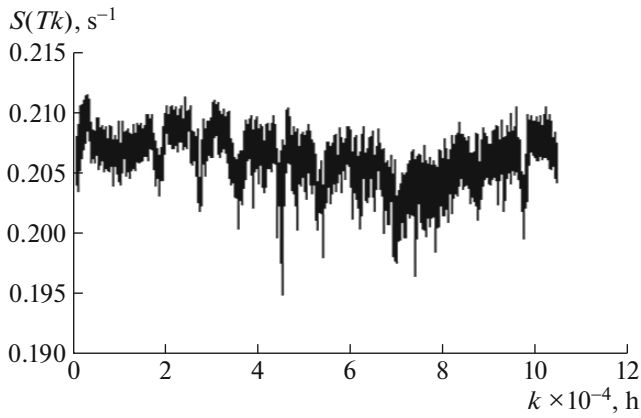


Fig. 1. Hourly averaged muon flux intensity function $S(Tk)$ plot for a 12-year interval.

periodicity of the $S(Tk)$ is clearly seen. The number of points in a year is, approximately, $N_y = 24 \times 30 \times 12 = 8640$, and the analyzed period includes about 12 annual oscillations of the considered intensity function. On Fig. 2, the plot for the $S(Tk)$ function for nearly a month corresponding to the time period June 29, 2015–July 31, 2015, between $k_1 = 74800$ and $k_2 = 75600$, is presented.

Figure 2 clearly displays the $S(Tk)$ function diurnal periodicity. As the number of points in the day is $N_c = 24$, the considered 800-point interval includes about 32 diurnal oscillations. Figure 1 nearly depicts the 11-year solar activity cycle waveform. It is known that the solar activity maximum was in 2014, to which the $S(Tk)$ minimum refers; the solar activity minimum was in 2008, to which the $S(Tk)$ maximum refers.

2.2. Frequency Domain Analysis

Let us analyze the oscillatory components in the data from MH using the frequency domain analysis.

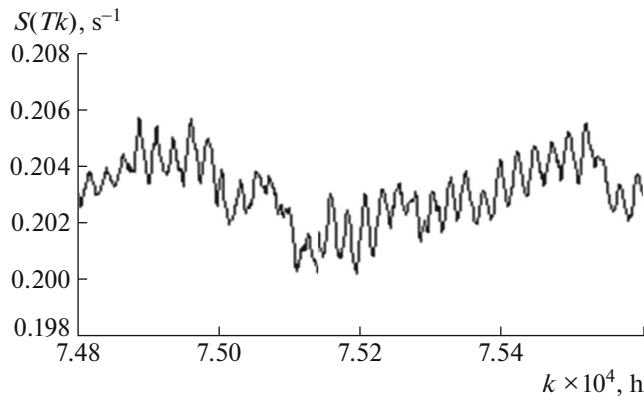


Fig. 2. Hourly averaged muon flux intensity function $S(Tk)$ plot for a 1-month interval.

Here we use the discrete Fourier transform (DFT). Let N be the number of points on which the DFT is performed. We calculate the complex DFT spectral coefficients $C_0(n)$:

$$C_0(n) = \frac{1}{N} \sum_{s=0}^{N-1} S(Ts) \exp(-jns/N),$$

where $n = 0, 1, \dots, N - 1$, and j denotes the imaginary unit for disambiguation.

For an easiest spectra visualization, we introduce a logarithmic scale $LC(n)$:

$$LC(n) = 20 \log_{10}(C(n)),$$

where $C(n) = C_0^*(n)C_0(n)$.

Let us calculate the spectral estimates. First we implement the sliding: $N_{1l} = N_0(l - 1) + 1$, $N_{2l} = N_{1l} + N - 1$, $l = 1, 2, \dots, m$, where N_0 is a sliding step. The spectrum resolution is $\Delta f = 1/NT$. The coefficients for the spectrum are the following:

$$C_l(n) = C_{0l}^*(n)C_{0l}(n),$$

$$C_{0l}(n) = \frac{1}{N} \sum_{n=N_{1l}}^{N_{2l}} S(Ts) \exp(-jns/N),$$

and the sum is $C(n) = \frac{1}{m} \sum_{l=1}^m C_l(n)$.

Let us assume, for example, $N = 16384 \times 4$, $N_0 = 4096$, and $m = 7$. The day period is $T_c = 24T$ seconds, and $f_c = 1/T_c = 1/24T$. Then, $n_c = f_c/\Delta f = NT/24T = 16384 \times 4/24 \approx 2731$ is the 1st harmonic number for a diurnal component. On Fig. 3, the calculated spectrum $LC(n)$ is presented, $n = 0, 1, \dots, 9999$.

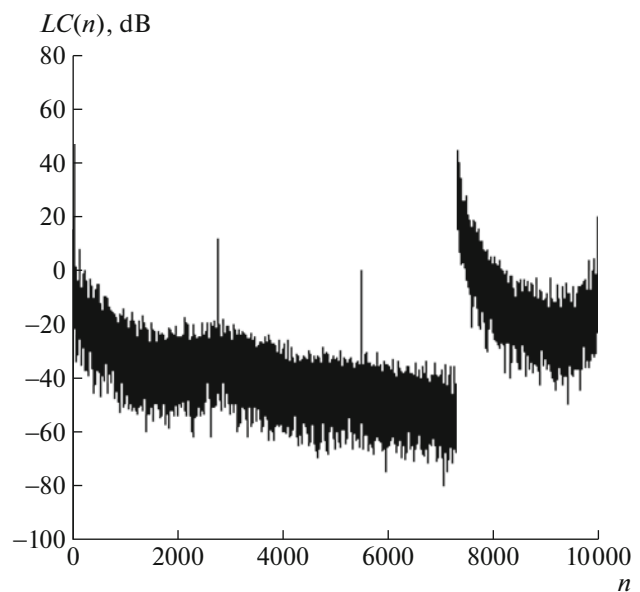


Fig. 3. The calculated spectrum $LC(n)$, $n = 0, 1, \dots, 9999$.

Three harmonics for the diurnal frequency are seen, and the 2nd and the 3rd harmonics are about 100 times smaller in amplitude than the first one.

For the annual component we calculate the number of the first harmonic. $T_y = 365 \times 24T$ seconds, $f_y = 1/T_y = 1/365 \times 24T$ and the 1st harmonic number for the annual component is $n_y = f_y/\Delta f = NT/T_y = 16384 \times 4/T_y \approx 7$. Figure 4 shows the calculated spectrum $LC(n)$, $n = 0, 1, \dots, 249$. The harmonics at 7, 14, and 21 can be easily seen.

It is seen that the harmonic, which determines the 11-year solar component, has the number $n_{s0} = 1$. For a more accurate spectral analysis of this component, it is necessary to have observations over a time interval of at least 50–100 years. The first harmonic number for the component associated with the rotation of the Sun, every 27 days, can be easily determined: $n_s = n_c/27 \approx 102$. It is easy to see that the amplitudes of these components are commensurate with the amplitudes of the diurnal components.

The considered observation of hourly MH matrices for the period 2007–2018 in the time and frequency domains confirms the presence of the indicated components. Let us assume that the average frequency of variations in the muon fluxes is generally lower than that of the diurnal ones but higher than that of the 27-day solar ones.

3. TWO-DIMENSIONAL BANDPASS FILTERING FOR MH MATRIX OBSERVATIONS

Let us consider eliminating the mentioned periodical components using digital two-dimensional bandpass filtering. According to our conclusions from the variation analysis, the relative cutoff frequencies for the applied filters will be $W_{c1} = \alpha_1/24 \times 27$, $W_{c2} = \alpha_2/24$, where $\alpha_1 \approx 1.05$ and $\alpha_2 \approx 0.95$ are the assignable coefficients. Let us select the Butterworth bandpass filter [11]. We will filter for each function $M_a(i, j, Tk)$, $k = 1, \dots, k_f$, and the total number of filtering operations will be N_1N_2 . We apply the standard procedures of digital one-dimensional filtering with weights, which are presented in general form— $b_r(i, j)$, $r = 1, \dots, r_0$, $a_s(i, j)$, $s = 0, \dots, s_0$; let us formulate the one-dimensional difference equation, where $M_{a,F}(i, j, Tk)$ is the digital filter output.

$$\begin{aligned}
 &M_{a,F}(i, j, Tk) \tag{1} \\
 &= - \sum_{r=1}^{r_0} b_r(i, j) M_{a,F}(i, j, T(k-r)) \\
 &+ \sum_{s=0}^{s_0} a_s(i, j) M_a(i, j, T(k-s)).
 \end{aligned}$$

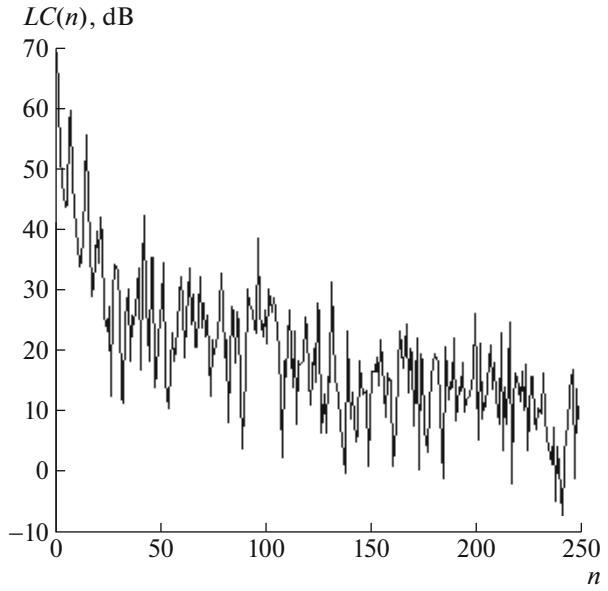


Fig. 4. The calculated spectrum $LC(n)$, $n = 0, 1, \dots, 249$. The peaks at $n = 7, 14,$ and 21 indicate the harmonics corresponding to the annual component.

The use of digital one-dimensional filters in the form of (1) for the task posed involves two problems: 1. the need to ensure small time costs to perform N_1N_2 one-dimensional filtering operations according to (1); 2. the need to eliminate the emerging phase shifts occurring in $M_{a,F}(i, j, Tk)$ due to the influence of recurrence relations in (1). We implement the filtering for the time series of matrices $M_a(Tk)$ from MH based on a two-stage approach.

At the first stage we will create the matrices $B_1, \dots, B_{r_0}, A_0, \dots, A_k$ consisting of weight elements b_r, a_s for (1). Using them, we form the two-dimensional filter structure based on the one-dimensional difference equation in the matrix form:

$$\begin{aligned}
 M_{a,F}(Tk) = & - \sum_{r=1}^{r_0} B_r \circ M_{a,F}(T(k-r)) \tag{2} \\
 & + \sum_{s=1}^{s_0} A_s \circ M_{a,F}(T(k-s)),
 \end{aligned}$$

where “ \circ ” denotes the Hadamar product (an operation of entrywise multiplication for matrices). Using the capabilities of Matlab, we realize the ultrafast elementwise multiplication of matrices. The matrix sequence $M_{a,F}(Tk)$ is the filter (2) output.

At the second stage, we will eliminate phase shifts. We introduce the function of total intensity $S_F(Tk)$ for $M_{a,F}(Tk)$. Let us form the functional $F(S, S_F, k_d)$ and find the optimal phase shift k_d°

$$k_d^\circ = \arg \left\{ \min_{1 \leq k_d \leq k_{d0}} F(S, S_F, k_d) \right\},$$

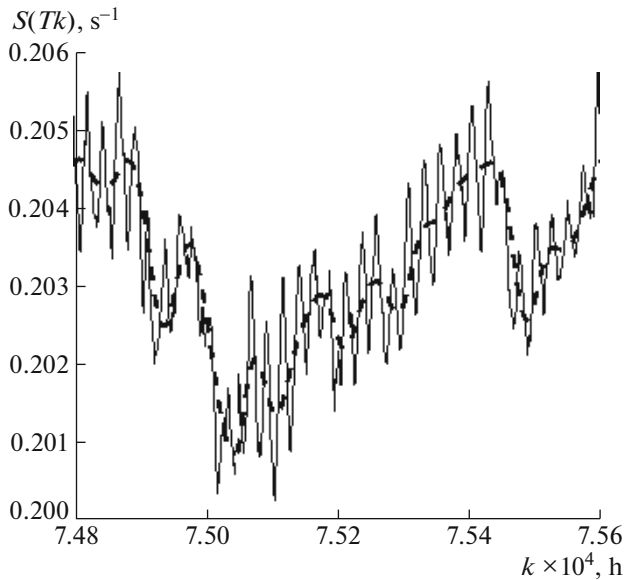


Fig. 5. The result of matrix data filtering—the elimination of diurnal variations for June 29–July 31, 2015. The result (solid line) is overlaid on the initial data for a better comparison.

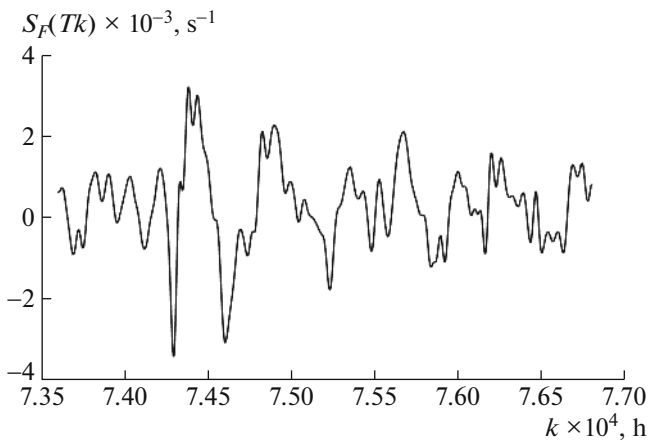


Fig. 6. The result of matrix data filtering (the elimination of diurnal, annual, solar 11-year and 27-day variations) for a 132-day period. The resulting curve contains only aperiodic muon flux variations.

where

$$S_F(Tk) = \frac{1}{N_1 N_2} \sum_{i=1}^{N_1} \sum_{j=1}^{N_2} M_{a,F}(i, j, Tk),$$

and

$$F(S, S_F, k_d) = \sum_{k=k_1}^{k_2} (S(Tk) - S_F(T(k - k_d)))^2. \tag{3}$$

The result of filtering at the second stage is defined as the sequence of matrices in which the shift correction is made k_d^0 : $M_{a,F0}(i, j, Tk) = M_{a,F}(i, j, T(k - k_d^0))$.

4. TESTING THE METHOD OF TWO-DIMENSIONAL BANDPASS FILTERING OF MH MATRIX DATA

For illustrative purposes, an example of eliminating diurnal variations in the MH matrix data was considered. A one-dimensional high-pass filter with a cutoff frequency $W_c = \alpha_2/24$ was used for filtering. Based on it, the $B_1, \dots, B_{r_0}, A_0, \dots, A_k$ matrices were created, consisting of the weight elements b_r, a_s for (1), and, using them, the two-dimensional filter (2) structure was formed, and the matrices $M_{a,F}(Tk)$ and the functions $M_{a,F}(i, j, Tk)$ were obtained. The phase shift was corrected based on (3) and the $M_{a,F0}(i, j, Tk)$ functions were formed.

On Fig. 5, the original function $S(Tk)$ and the filtering result $S_{F0}(Tk), k = 1, \dots, k_f$ (solid line), formed from the function $M_{a,F0}(i, j, Tk)$ set are shown for the period of time June 29, 2015–July 31, 2015. It is seen that the daily components in the matrix data were eliminated.

It was established on the basis of computational experiments that: the time spent on the proposed filtering method with an appropriate ratio of N_1, N_2, k_f parameters is on average 5–10 times less than the time spent for filtering on the basis of one-dimensional filters; errors in estimating phase shifts are about 1° to 2° .

The elimination of periodic diurnal, annual, solar 27-day and 11-year variations in the MH matrix observation data was implemented. A bandpass filter with cutoff frequencies. $W_{c1} = \alpha_1/24 \times 27, W_{c2} = \alpha_2/24$ was applied. Figure 6 shows the filtering result for the interval within the points $k_1 = 73600, k_2 = 76800$ (132 days). In the filtered function $S_{F0}(Tk)$, only aperiodic MF variations were left.

5. CONCLUSIONS

1. The proposed method for eliminating periodic diurnal, annual, and solar variations in the matrix observations of the URAGAN muon hodoscope based on two-dimensional band-pass filtering appeared to be workable.

2. It is established on the basis of computational experiments that: the time costs of the proposed filtering method, with appropriate ratios of parameters, are on average 5–10 times less than the time spent for filtering on the basis of one-dimensional filters. Phase shift correction errors are of the order of 1° – 2° .

3. The proposed method can be applied to many problems of experimental physics, associated with the elimination in the sequences of matrix observations of the components of periodic variations.

ACKNOWLEDGMENTS

This work was supported by a grant from the Russian Science Foundation no. 17-17-01215.

REFERENCES

1. I. I. Yashin, I. I. Astapov, N. S. Barbashina, V. V. Borog, D. V. Chernov, A. N. Dmitrieva, R. P. Kokoulin, K. G. Kompaniets, Yu. N. Mishutina, A. A. Petrukhin, V. V. Shutenko, and E. I. Yakovleva, *Adv. Space Res.* **56**, 2693 (2015).
2. *NEVOD complex* (National Research Nuclear University MEPhI), www.nevod.mephi.ru.
3. *Two-dimensional Signal Analysis* (Ed. by R. Garello, 2013), p. 352.
4. J. W. Woods, *Multidimensional Signal, Image, and Video Processing and Coding* (Academic Press, 2012).
5. J. Poirier and T. Catanach, in *Proceeding of the 32nd International Cosmic Ray Conference, Beijing, 2011*, Vol. 11, p. 173.
6. Y. Okazaki, A. Fushishita, T. Narumi, C. Kato, S. Yasue, T. Kuwabara, J. W. Bieber, P. Evenson, M. R. Da Silva, A. Dal Lago, N. J. Schuch, Z. Fujii, M. L. Duldig, J. E. Humble, I. Sabbah, J. Kóta, and K. Munakata, *Astrophys. J.* **681**, 693 (2008).
7. I. Braun, J. Engler, J. R. Hörandel, and J. Milke, *Adv. Space Res.* **43**, 480 (2009).
8. G. G. Karapetyan, *Phys. Rev. D* **89**, 093005 (2014).
9. A. N. Dmitrieva, R. P. Kokoulin, A. A. Petrukhin, and D. A. Timashkov, *Astropart. Phys.* **34**, 401 (2011).
10. R. V. Sidorov, I. I. Astapov, N. S. Barbashina, A. D. Gvishiani, V. G. Getmanov, A. N. Dmitrieva, M. N. Dobrovolsky, D. V. Peregoudov, A. A. Soloviev, V. E. Chinkin, V. V. Shutenko, and I. I. Yashin, *Bull. Russ. Acad. Sci. Phys.* **83**, 650 (2019).
11. *Filter Design Matlab Toolbox*.
<http://matlab.exponenta.ru>.